

# Insight into the Electronic Structure, Optical Properties, And Redox Behavior of the Hybrid Phthalocyaninoclathrochelates from Experimental and Density Functional Theory Approaches

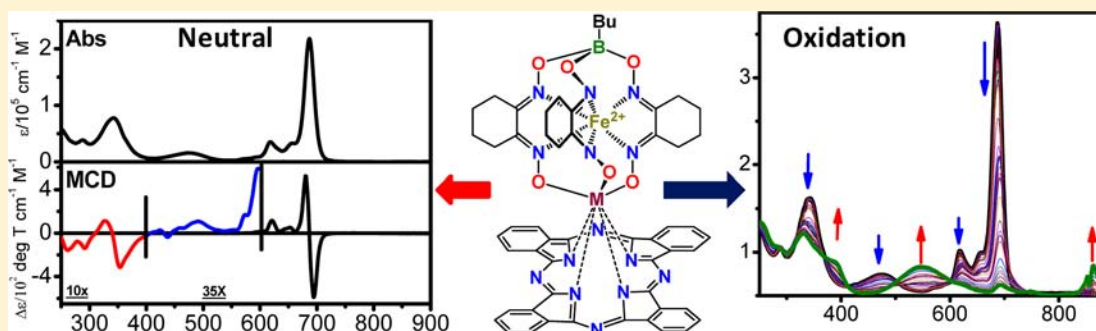
Jared R. Sabin,<sup>†</sup> Oleg A. Varzatskii,<sup>‡</sup> Yan Z. Voloshin,<sup>\*,§</sup> Zoya A. Starikova,<sup>§</sup> Valentin V. Novikov,<sup>§</sup> and Victor N. Nemykin<sup>\*,†</sup>

<sup>†</sup>Department of Chemistry & Biochemistry, 1039 University Drive, University of Minnesota Duluth, Duluth, Minnesota 55812, United States

<sup>‡</sup>Vernadskii Institute of General and Inorganic Chemistry, National Academy of Sciences of Ukraine, 03680 Kiev, Ukraine

<sup>§</sup>Nesmeyanov Institute of Organoelement Compounds, Russian Academy of Sciences, 11991 Moscow, Russia

## Supporting Information



**ABSTRACT:** An insight into the electronic structure of several hafnium(IV), zirconium(IV), and lutetium(III) phthalocyaninoclathrochelates has been discussed on the basis of experimental UV-vis, MCD, electro- and spectroelectrochemical data as well as density functional theory (DFT) and time-dependent DFT (TDDFT) calculations. On the basis of UV-vis and MCD spectroscopy as well as theoretical predictions, it was concluded that the electronic structure of the phthalocyaninoclathrochelates can be described in the first approximation as a superposition of the weakly interacting phthalocyanine and clathrochelate substituents. Spectroelectrochemical data and DFT calculations clearly confirm that the highest occupied molecular orbital (HOMO) in all tested complexes is localized on the phthalocyanine ligand. X-ray crystallography on zirconium(IV) and earlier reported hafnium(IV) phthalocyaninoclathrochelate complexes revealed a slightly distorted phthalocyanine conformation with seven-coordinated metal center positioned  $\sim 1$  Å above macrocyclic cavity. The geometry of the encapsulated iron(II) ion in the clathrochelate fragment was found to be between trigonal-prismatic and trigonal-antiprismatic.

## 1. INTRODUCTION

Supramolecular assemblies with several electronically coupled transition-metal centers have been intensively investigated during the past several decades because of their potential application in molecular electronics and light-harvesting modules.<sup>1–5</sup> Hybrid inorganic and organometallic transition-metal arrays with relatively isolated  $\pi$ - and  $\sigma$ -electronic fragments, which belong to different substituents, on the other hand, have received relatively little attention. Such “polytopic” materials, however, have proven to be a potentially useful building blocks for redox- and photoredox driven molecular electronic devices as well as artificial photosynthetic systems with long-lived charge separation states.<sup>6,7</sup> Of the published reports on polytopic transition-metal complexes, the recently discovered phthalocyaninoclathrochelates<sup>8,9</sup> deserve special attention. These phthalocyanine-capped cage iron(II)

hybrid complexes have a phthalocyanine-centered extensive  $\pi$ -system that is coupled to the  $\sigma$ -bonded transition-metal cage. While phthalocyanine  $\pi$ -systems could be exploited for their known photo- and electro-chromic as well as photocatalytic properties,<sup>10</sup> complementary iron(II) chlathrochelate fragments could be utilized as sensitizers in photochemical hydrogen production from water.<sup>11</sup> So far, several zirconium(IV), hafnium(IV), and lutetium phthalocyaninoclathrochelates have been prepared and characterized by spectroscopic and electrochemical methods.<sup>8,9</sup> Although significant progress has been made in synthesis and characterization of the phthalocyaninoclathrochelates, little is known about their electronic structure as well as UV-vis spectra band assign-

Received: April 30, 2012

Published: July 16, 2012

ments. Moreover, all electrochemical data were assigned on the basis of the available literature data for parent phthalocyanines<sup>12</sup> and clathrochelates<sup>13</sup> and have not been confirmed by experimental and theoretical methods.

Thus, in this paper, electronic structure and experimental UV–vis band assignments of several phthalocyaninoclathrochelates (Figure 1) are discussed on the basis of density

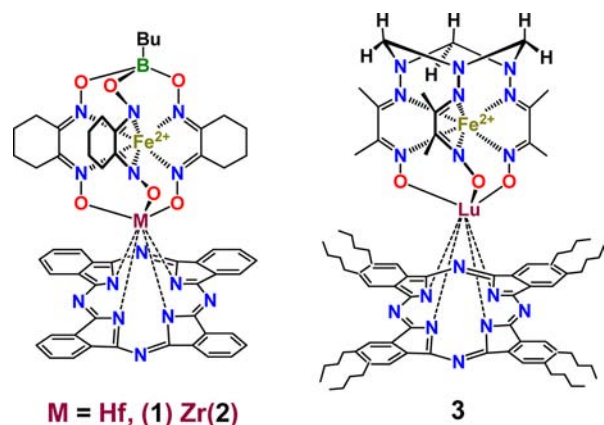


Figure 1. Target phthalocyaninoclathrochelate complexes.

functional theory (DFT) and time-dependent DFT (TDDFT) approaches. In addition, theoretical findings were supported by magnetic circular dichroism (MCD) and spectroelectrochemical data. Finally, a new X-ray structure of the zirconium(IV) phthalocyaninoclathrochelate is also reported.

## 2. EXPERIMENTAL SECTION

**Materials and Physical Measurements.** Dichloromethane (DCM) was distilled over calcium hydride prior to experiments. For electrochemical experiments, tetrabutylammonium perchlorate (TBAP) was recrystallized twice from ethyl acetate. UV–vis data were obtained on Jasco-720 or Cary 17 spectrophotometers. MCD data were recorded using OLIS DCM 17 CD spectropolarimeter using 1.4 T DeSa magnet. The MCD spectra were measured in  $mdeg = [\theta]$  and converted to  $\Delta\epsilon$  ( $M^{-1} cm^{-1} T^{-1}$ ) using the regular conversion formula:  $\Delta\epsilon = \theta / (32980 \times Bdc)$ , where  $B$  is the magnetic field,  $d$  is the path length, and  $c$  is the concentration. Complete spectra were recorded at room temperature in parallel and antiparallel directions with respect to the magnetic field. Electrochemical measurements were conducted using a CH electrochemical analyzer utilizing a three-electrode scheme with platinum working, auxiliary, and Ag/AgCl reference electrodes in 0.1 M solution of TBAP in DCM with redox potentials corrected using an internal standard (ferrocene) in all cases. Spectroelectrochemical data were collected using a home-built spectroelectrochemical cell in 0.3 M solution of TBAP in DCM.

**Computational Details.** All computations were performed using Gaussian 03 or Gaussian 09<sup>14</sup> software packages running under Windows or UNIX OS. The excitation energies were calculated by a TDDFT approach with the lowest 100 singlet excited states considered to ensure that both *Q*- and *B*-band regions of the UV–vis spectra of phthalocyaninoclathrochelates are covered. Theoretical spectra were modeled using GaussView 5.0 software<sup>15</sup> using a 800  $cm^{-1}$  bandwidth in all cases. In all geometry optimizations, Becke's exchange functional<sup>16</sup> and Perdew's correlation functional<sup>17</sup> (BP86) were used. All complexes were optimized without any truncations in geometry except B-Bu groups in complexes 1 and 2 were modeled using B-Me substituents. For all optimized geometries, vibronic frequencies were calculated to confirm minima on the potential energy surface of corresponding phthalocyaninoclathrochelates. Taking into consideration the size of the phthalocyaninoclathrochelates, ECP LANL2DZ basis set<sup>18</sup> was used for all atoms. Single point and

TDDFT calculations were conducted using pure GGA BP86, hybrid B3LYP<sup>19</sup> and long-range corrected CAM-B3LYP<sup>20</sup> exchange-correlation functionals. During testing of all exchange-correlation functionals, it has been found that the “standard” GGA (BP86) and hybrid (B3LYP) functionals predict the number of intense charge-transfer transitions in the *Q*-band region of phthalocyaninoclathrochelates, which is inconsistent with the experimental data. Use of the long-range corrected CAM-B3LYP exchange-correlation functional, however, resulted in much better correlation between the experimental data and the theoretical results for the target compounds. The percentage of atomic orbital contributions to their respective molecular orbitals were calculated by using the VMOdes program.<sup>21</sup> Since the low-spin state of iron(II) ion in clathrochelate substituent of complexes 1–3 (as well as all known iron(II) clathrochelates) has clearly been established on the basis of polynuclear NMR and Mössbauer spectroscopies,<sup>8,9</sup> only the diamagnetic ground states were considered in DFT and TDDFT calculations.

**Single Crystal X-ray Analysis.** Single crystals of complex 2 were grown at room temperature using a benzene–isooctane mixture. The crystallographic measurements were conducted at 120 (2) K using Bruker SMART 1 K CCD area detector and Mo- $K\alpha$  radiation ( $\lambda = 0.71073 \text{ \AA}$ ).<sup>22</sup> Reflection intensities were integrated using SAINT software and corrected by a semiempirical method (SADABS program).<sup>23</sup>

The structure was solved by the direct method and refined by full-matrix least-squares in the anisotropic approximation for nonhydrogen atoms using SHELXTL.<sup>24</sup> Positions of the hydrogen atoms were calculated geometrically and refined using the riding model with isotropic temperature factors  $U_{iso} = nU_{eq}(C)$ , where  $n = 1.5$  for methyl groups and 1.2 for the others;  $U_{eq}$  values are the equivalent isotropic displacements parameters of the corresponding pivot carbon atoms. Crystal data for  $FeN_3(Bu-C_4H_9)(ZrPc) \cdot 3C_6H_6$ :  $C_{72}H_{66}BN_{14}O_6FeZr$ ,  $M = 1382.28$ , monoclinic, crystal size  $0.60 \times 0.44 \times 0.20 \text{ mm}$ , space group  $P2_1/c$ ,  $a = 20.570(3)$ ,  $b = 12.248(2)$ ,  $c = 26.966(3) \text{ \AA}$ ,  $\beta = 107.766(4)^\circ$ ,  $V = 6469.5(2) \text{ \AA}^3$ ,  $Z = 4$ ,  $\rho_{calcd} = 1.419 \text{ g}\cdot\text{cm}^{-3}$ ,  $2\theta_{max} = 52.00^\circ$ , 12572 unique data ( $R_{int} = 0.1087$ ),  $R_1 = 0.0675$  (8804 refls. with  $I > 2\sigma(I)$ ),  $R_w = 0.1392$  (all unique reflections), number of parameters: 820, GOF = 1.011. CCDC reference number is 780361. The main geometrical parameters of the molecule are represented in Table 1.

## 3. RESULTS AND DISCUSSION

**UV–vis and MCD Spectra of Selected Phthalocyaninoclathrochelates.** UV–vis and MCD spectra of selected phthalocyaninoclathrochelates are shown in Figure 2. In the first approximation, the degree of electronic interaction between the porphyrinoid-type chromophore and axially coordinated ligand(s) could be determined using UV–vis spectra of such assemblies. When axial ligand(s) are electronically coupled with porphyrinoid-type chromophores, then their most prominent *B*- (Soret-) and *Q*-bands undergo significant shifts to the lower or higher energy regions.<sup>5,25</sup> When the degree of electronic interaction between the porphyrinoid-type chromophore and the axial ligand(s) is small, however, then the energies of its most prominent *B*- (Soret-) and *Q*-bands will remain close to those observed in the parent chromophore.<sup>26</sup> UV–vis spectra of selected phthalocyaninoclathrochelates could be clearly viewed as a superposition of the UV–vis spectra of the parent phthalocyanine chromophores and the axial clathrochelate ligands. UV–vis spectra of phthalocyaninoclathrochelates are dominated by the intense *Q*- and *B*-band regions with the corresponding observed maxima at 687–688 and 342–350 nm. Both *Q*- and *B*-band regions of the phthalocyaninoclathrochelates are virtually indistinguishable ( $\pm 2 \text{ nm}$ ) from the UV–vis spectra of the respective parent hafnium, zirconium, and lutetium phthalocyanines.<sup>26</sup> Broad bands, which are observed at 474–480 nm for hafnium and

**Table 1.** Selected Bond Distances and Angles in Zirconium(IV)-Capped Complex 2 According to X-ray Diffraction Data

| Bond Distances (Å) |          |             |                             |
|--------------------|----------|-------------|-----------------------------|
| Zr1–O2             | 2.092(3) | Fe1–N1      | 1.905(3)                    |
| Zr1–O4             | 2.095(3) | Fe1–N3      | 1.903(3)                    |
| Zr1–O6             | 2.115(3) | Fe1–N5      | 1.896(3)                    |
| Zr1–N8             | 2.257(4) | Fe1–N2      | 1.927(3)                    |
| Zr1–N10            | 2.259(4) | Fe1–N4      | 1.913(3)                    |
| Zr1–N12            | 2.266(4) | Fe1–N6      | 1.920(3)                    |
| Zr1–N14            | 2.262(3) | O1–N1       | 1.390(4)                    |
| O2–N2              | 1.364(4) | O3–N3       | 1.373(4)                    |
| O4–N4              | 1.371(4) | O5–N5       | 1.372(4)                    |
| O6–N6              | 1.347(4) | N1–C1       | 1.297(5)                    |
| N2–C2              | 1.294(5) | N3–C3       | 1.305(5)                    |
| N4–C4              | 1.305(5) | N5–C5       | 1.305(5)                    |
| N6–C6              | 1.306(5) | C3–C4       | 1.439(6)                    |
| C1–C2              | 1.443(5) | N1...N3     | 2.597(5)                    |
| C5–C6              | 1.441(6) | N3...N5     | 2.611(5)                    |
| N1...N5            | 2.583(5) | N2...N6     | 2.670(5)                    |
| N2...N4            | 2.695(5) | N4...N6     | 2.714(5)                    |
| Angles (deg)       |          |             |                             |
| N3–Fe1–N5          | 86.8(1)  | N1–Fe1–N3   | 86.0(1)                     |
| N1–Fe1–N2          | 78.5(1)  | N1–Fe1–N5   | 85.6(1)                     |
| N3–Fe1–N4          | 79.0(1)  | N2–Fe1–N4   | 89.2(1)                     |
| N5–Fe1–N6          | 79.4(1)  | N2–Fe1–N6   | 87.9(1)                     |
| O2–Zr1–O4          | 83.7(1)  | N4–Fe1–N6   | 90.2(1)                     |
| O6–Zr1–O4          | 84.6(1)  | O1–B1–O3    | 109.2(3)                    |
| O2–Zr1–O6          | 82.6(1)  | O1–B1–O5    | 109.2(3)                    |
| N2–O2–Zr1          | 123.5(2) | O3–B1–O5    | 110.0(3)                    |
| N4–O4–Zr1          | 124.0(2) | C1–N1–O1    | 116.5(3)                    |
| N6–O6–Zr1          | 124.5(2) | C3–N3–O3    | 117.0(3)                    |
| N1–O1–B1           | 111.2(3) | C5–N5–O5    | 116.8(3)                    |
| N3–O3–B1           | 111.3(3) | C4–N4–O4    | 115.5(3)                    |
| N5–O5–B1           | 111.5(3) | Fe1–N2–O2   | 125.6(3)                    |
| C2–N2–O2           | 116.2(3) | Fe1–N4–O4   | 125.9(2)                    |
| Fe1–N1–O1          | 123.2(2) | Fe1–N6–O6   | 124.9(2)                    |
| Fe1–N3–O3          | 123.7(2) | <i>h</i> /Å | 2.295                       |
| Fe1–N5–O5          | 123.5(2) | $\varphi$   | 30.1, 30.1, 30.4 (av. 30.2) |
| C6–N6–O6           | 117.2(3) | $\alpha$    | 39.5                        |

zirconium complexes **1** and **2**, as well as a broad unstructured band observed between  $\sim 500$  and  $600$  nm for lutetium complex **3**, are virtually identical to the UV-vis spectra of the starting iron(II) clathrochelates<sup>27</sup> except in the latter case, where some of the low-energy charge-transfer bands are masked by more intense vibronic satellites of the phthalocyanine-centered Q-band observed between  $600$  and  $650$  nm. MCD spectra of complexes **1–3** are dominated by the very intense phthalocyanine-centered Q-band represented by the Faraday A-term centered between  $687$  and  $690$  nm (Figures 2–4). In agreement with perimeter model<sup>28</sup> and earlier MCD data on phthalocyanines,<sup>29</sup> another (about one order of magnitude smaller) Faraday A-term was observed in the B-band region ( $340$ – $348$  nm). Intensities of the MCD signals of the charge-transfer transitions in iron(II) clathrochelate substituents are expected to be significantly smaller compared to intensities of phthalocyanine-centered  $\pi$ – $\pi^*$  transitions.<sup>28,30</sup>

In agreement with this expectation, we had to collect MCD data on clathrochelate-centered charge-transfer transitions in  $400$ – $600$  nm region using  $\sim 10$  times higher concentration of phthalocyaninoclathrochelates (Figure 2). MCD spectra of

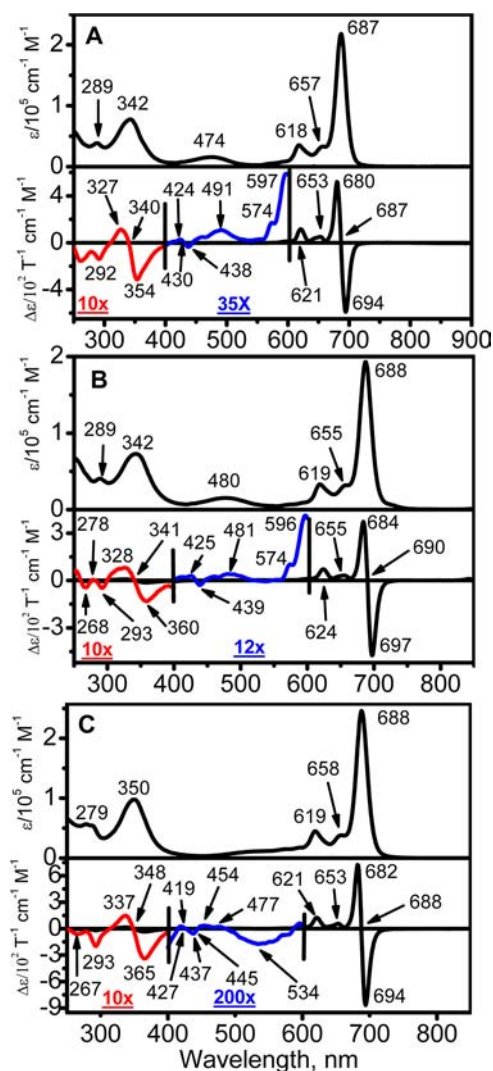


**Figure 2.** UV-vis (top) and MCD (bottom) spectra of hafnium(IV)-capped complex **1** (A), zirconium(IV)-capped complex **2** (B), and lutetium(III)-capped complex **3** (C), in DCM. Magnification of the MCD spectra in MLCT and B-band regions are color coded by red and blue fonts.

hafnium and zirconium complexes **1** and **2** in the  $400$ – $600$  nm region are very close to each other and consist of four major features. The highest energy feature is the Faraday A-term centered at  $430$  nm. Since the same feature is present at the same energy in phthalocyaninoclathrochelate lutetium complex **3** as well as nickel tetra-*tert*-butyl-phthalocyanine complex (Supporting Information, Figure 1), this Faraday A-term was assigned to the second doubly degenerate  $^1E$  ( $C_{4v}$  effective symmetry of phthalocyanine chromophore) excited state predicted earlier by semiempirical<sup>31</sup> and TDDFT<sup>32</sup> calculations on simple main group and transition-metal phthalocyanines and confirmed below on the basis of TDDFT calculations on phthalocyaninoclathrochelates.

Two lowest energy positive Faraday B-terms observed at  $\sim 575$  and  $595$  nm could be easily attributed to typical for the phthalocyanine compounds<sup>33</sup> vibronic components of the  $Q_{0-0}$  band centered at  $687$ – $688$  nm in complexes **1** and **2**. Two positive Faraday B-terms observed at  $454$  and  $480$  nm were attributed to the predominantly clathrochelate-centered as well as clathrochelate-to-phthalocyanine and phthalocyanine-to-

clathrochelate charge-transfer bands based on the experimental UV–vis spectra of iron(II) clathrochelates and the TDDFT calculations on phthalocyaninoclathrochelates discussed below. Similar to the MCD spectra of complexes **1** and **2**, the MCD spectrum of lutetium phthalocyaninoclathrochelate **3** in the 400–600 nm region has a weak Faraday *A*-term centered at 427 nm, which could be attributed to the second doubly degenerate <sup>1</sup>E state ( $C_{4v}$  effective symmetry) of the phthalocyanine chromophore. The charge-transfer region of the clathrochelate substituent in complex **3** is presented by two weak positive Faraday *B*-terms observed at 454 and 477 nm and one more intense and very broad negative Faraday *B*-term centered at 480 nm. This negative *B*-term overlaps with two positive Faraday *B*-terms located at 575 and 595 nm resulting in reduced intensity of the latter signal and negative amplitude of the former one. Both signals can be attributed to the vibronic components of the intense phthalocyanine-centered  $Q_{0-0}$  band observed as a Faraday *A*-term at 688 nm. On the other hand, Faraday *B*-terms observed at 454, 477, and 480 nm could be attributed to the predominantly intraligand clathrochelate-centered charge-transfer transitions as discussed below. Overall, UV–vis and MCD data for phthalocyaninoclathrochelate complexes **1–3**, in the first approximation, could be interpreted in the terms of an electronically uncoupled system, which consists of phthalocyanine and clathrochelate chromophores.

#### X-ray Structure of Phthalocyaninoclathrochelate **2**.

The molecular structure of the phthalocyaninoclathrochelate **2** is shown in Figure 3. The first coordination sphere of the  $FeN_6$

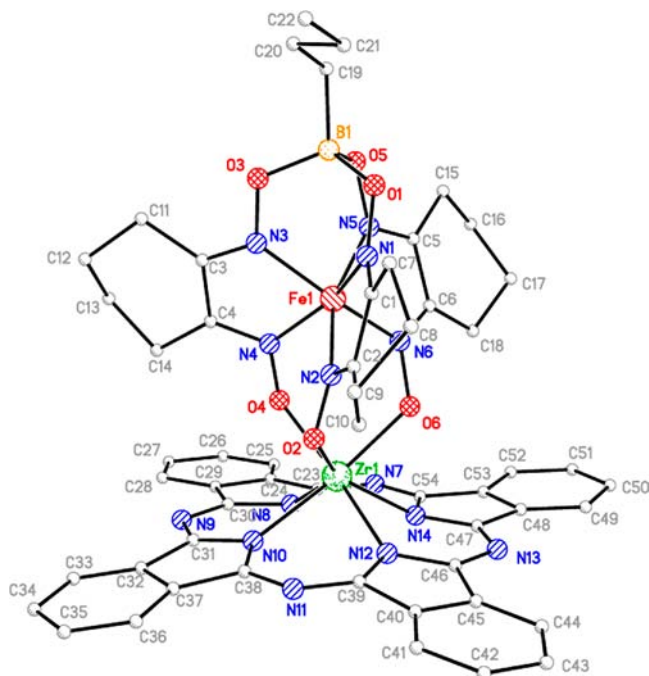


**Figure 3.** X-ray structure of the zirconium(IV)-capped phthalocyaninoclathrochelate **2**. Hydrogen atoms are omitted for clarity.

polyhedron is in between a trigonal prism (TP, distortion angle  $\varphi = 0^\circ$ ) and a trigonal antiprism (TAP,  $\varphi = 60^\circ$ ): the angle  $\varphi$  value is equal to  $30.20^\circ$  and the height ( $h$ ) of this coordination polyhedron is approximately  $2.30 \text{ \AA}$ . These values are similar to those reported earlier for hafnium(IV) phthalocyaninoclathrochelate **1**.<sup>8</sup> The average Fe–N distance ( $1.91 \text{ \AA}$ ) is characteristic of the tris-dioximate iron(II) clathrochelates,<sup>11,34</sup> but the

Fe–N(2,4,6) bond lengths (av.  $1.92 \text{ \AA}$ ) for the zirconium-containing tripodal fragment are greater than those for the boron-capped moiety (the Fe–N(1,3,5) distances are approximately  $1.90 \text{ \AA}$ , Table 1).

The average bite angle  $\alpha$  (half of the N–Fe–N angle in chelate cycle) value is also characteristic of the macrobicyclic iron(II) tris-dioximates,<sup>11,34</sup> whereas the angles in the N–Fe–N fragments, in which donor nitrogen atoms belong to the different ribbed  $\alpha$ -dioximate fragments, are significantly higher in the case of the zirconium-capped moiety (av.  $89.1^\circ$ ) than those in the boron-containing one (av.  $86.3^\circ$ ). The distances of the encapsulated iron(II) ion to the planes defined by N1, N3, and N5 and N2, N4, N6 are  $1.126(2)$  and  $1.169(2) \text{ \AA}$ , respectively, and the average nonbonding N...N distances in these bases of the TP–TAP coordination polyhedron are equal to  $2.693(5)$  and  $2.597(5) \text{ \AA}$ , respectively. As a result, the O2–N2–Fe1–N4–O4 and O2–N2–Fe1–N6–O6 moieties are more open than the corresponding boron cross-linked fragments, and the N–O–B bond angles are more acute than the N–O–Zr angles with the remaining of the main geometrical parameters (the C=N, N–O, and C–C bond distances and the corresponding bond angles) in the  $\alpha$ -dioximate chelate cycles of the clathrochelate framework. These distortions of the mixed boronzirconium-capped clathrochelate framework may be caused by the difference in the (Shannon) radii<sup>35</sup> of its cross-linking ions as well as by their different Lewis acidity. Similar to the earlier reported ditopic complex **1**,<sup>8</sup> the phthalocyanine ligand in complex **2** is slightly nonplanar with both hafnium and zirconium in **1** and **2** located at  $\sim 1 \text{ \AA}$  above the phthalocyanine central cavity. Both hafnium and zirconium centers in complexes **1** and **2** are seven-coordinated with four nitrogen atoms of phthalocyanine and three oxygen atoms of clathrochelate ligand. The average M–N bond distances observed for the zirconium complex **2** ( $2.26 \text{ \AA}$ ) are close to those found in the hafnium analogue **1** ( $2.24 \text{ \AA}$ ).<sup>8</sup> Similarly, average M–O bond distances observed in zirconium complex **2** ( $2.10 \text{ \AA}$ ) are close to those reported earlier for hafnium analogue **1** ( $2.09 \text{ \AA}$ , Table 1).<sup>8</sup>

The packing of the phthalocyaninoclathrochelate **2** and the major intermolecular interactions in this compound are very similar to those observed in the previously described hafnium-containing analogue **1**.<sup>8</sup> Specifically, only partial  $\pi$ – $\pi$  interactions were observed between neighboring phthalocyanine ligands with the closest contacts observed between the pyrrole units close to  $3.5 \text{ \AA}$ .

#### Electronic Structures and TDDFT Predicted Vertical Excitation Energies of Phthalocyaninoclathrochelates.

To gain a further insight into the UV–vis and MCD spectroscopy as well as the redox properties of phthalocyaninoclathrochelate complexes **1–3**, we investigated electronic structures and origins of the vertical excitation energies using DFT and TDDFT approaches, which are proven to provide accurate electronic structures and spectroscopic parameters for inorganic,<sup>36</sup> organometallic,<sup>37</sup> and organic compounds including porphyrinoids<sup>32,38</sup> and clathrochelates.<sup>39</sup> From spectroscopic and theoretical points of view, phthalocyaninoclathrochelate complexes **1–3** present an interesting case in which the axial clathrochelate ligand, with an effective 3-fold symmetry, is axially coordinated to the phthalocyanine chromophore with effective 4-fold symmetry. In agreement with X-ray data on zirconium and hafnium complexes **1** and **2**, all target compounds were optimized in the  $C_1$  point group, while all our attempts to increase the total symmetry to  $C_s$

resulted in imaginary frequencies indicative of structure instability. When comparison between theory and X-ray experiments is possible (Supporting Information, Table 1), it suggests that the DFT predicted geometries are in a good agreement with experimental parameters.

The DFT predicted MO diagrams for the target phthalocyaninoclathrochelates 1–3 are presented in Figure 4, while an analysis of the orbital compositions is provided in

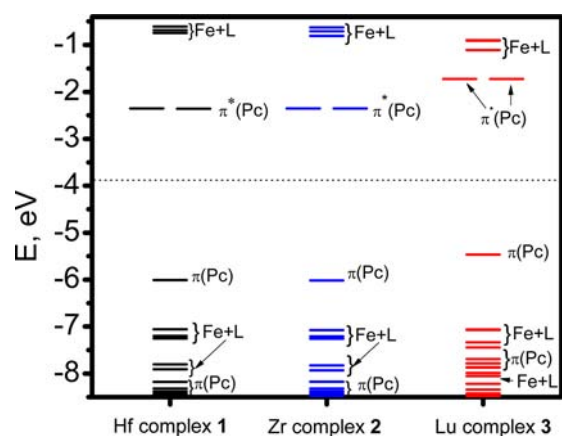


**Figure 4.** Molecular orbital energies of phthalocyaninoclathrochelates 1–3 (calculated at CAM-B3LYP/LANL2DZ level).

Supporting Information, Figure 2. The frontier orbitals of the target ditopic complexes 1–3 are pictured in Figure 5. In

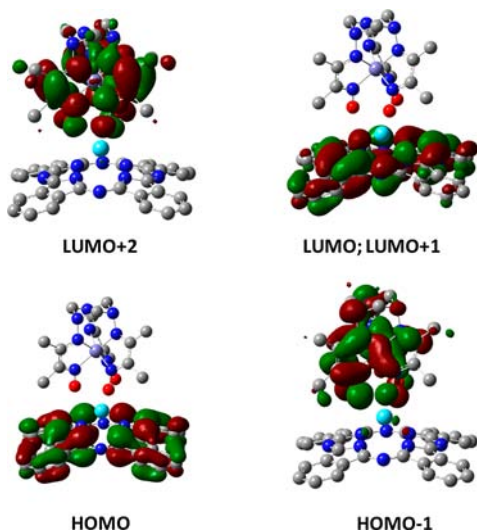


**Figure 5.** Frontier orbitals of phthalocyaninoclathrochelate 3 calculated at CAM-B3LYP/LANL2DZ level.

agreement with Gouterman's classic four-orbital model for porphyrins and phthalocyanines,<sup>40</sup> the highest occupied molecular orbital (HOMO) in complexes 1–3 is a phthalocyanine-centered  $\pi$ -orbital corresponding to an  $a_{1u}$  MO in the  $D_{4h}$  point group notation, which is reflective of the effective 4-fold symmetry of the phthalocyanine ligand. The HOMO in ditopic complexes 1–3 is a pure phthalocyanine-centered MO without any contribution from the axial clathrochelate ligand. Introduction of a single clathrochelate substituent into the phthalocyanine axial position in complexes 1 and 2 results in the next five MOs (HOMO-1 to HOMO-5)

becoming predominantly mixed iron ( $d_{xy}$ ,  $d_{x^2-y^2}$ , and  $d_z^2$ ) and clathrochelate  $\pi$  MOs, while the second classic Gouterman's phthalocyanine-centered occupied  $\pi$ -orbital of  $a_{2u}$  symmetry ( $D_{4h}$  point group) is located at the lower energy (HOMO-6).

The different nature of the clathrochelate ligand in complex 3 leads to situation when the classic phthalocyanine-centered Gouterman's  $\pi$ -orbitals are separated by only three (HOMO-1 to HOMO-3) mixed clathrochelate/iron MOs, with two of them (HOMO-1 and HOMO-2) being nearly degenerate (Figure 4). In agreement with previous computational data<sup>31,32,38</sup> as well as the classic Gouterman's model,<sup>40</sup> the nearly degenerate lowest unoccupied molecular orbital (LUMO) and LUMO+1 in ditopic complexes 1–3 are pure phthalocyanine-centered  $\pi$ -orbitals with no admixture from the axial clathrochelate ligand. In zirconium and hafnium ditopic complexes 1 and 2, these MOs are energetically well separated from the higher energy, clathrochelate-centered unoccupied  $\pi^*$ -orbitals (LUMO+2 to LUMO+4). The energies of clathrochelate-centered unoccupied  $\pi^*$ -orbitals (LUMO+2 to LUMO+4) in complex 3, however, are much closer to the phthalocyanine-centered LUMO and LUMO+1 (Figure 4). Because of the redox silent nature and size similarities of the hafnium and zirconium ions in complexes 1 and 2, it is expected that the orbital energies and compositions of MOs in these compounds should be very close to each other and indeed, analysis of the MO compositions and energies confirms this hypothesis. Taking into consideration the large metal–metal distances in complexes 1–3, it is not surprising to see that the long-range corrected DFT calculations predict no significant overlap between two metalcenters. The electron-donating properties of the clathrochelate substituent in complex 3 result in significantly higher energies of the phthalocyanine-centered classic Gouterman's  $\pi$ -orbitals compared to those in complexes 1 and 2, and this trend is in excellent agreement with the electrochemical data on the respective phthalocyaninoclathrochelates.<sup>8,9</sup>

Overall, based on the DFT predicted electronic structure of the phthalocyaninoclathrochelates 1–3, one would expect the following classes of electronic transitions in their UV–vis and MCD spectra: (i) phthalocyanine-centered intra-ligand  $\pi$ – $\pi^*$  transitions; (ii) clathrochelate-centered d-d, metal-to-ligand charge-transfer (MLCT), and ligand-to-metal charge transfer (LMCT) transitions; (iii) phthalocyanine-to-clathrochelate inter-ligand LMCT and  $\pi$ – $\pi^*$  transitions; (iv) clathrochelate-to-phthalocyanine MLCT and  $\pi$ – $\pi^*$  transitions (Figure 6). In the oversimplified picture, it is expected that the phthalocyanine-centered  $\pi$ – $\pi^*$  transitions to the nearly degenerate LUMO and LUMO+1 will result in intense absorption bands observed in UV–vis spectra as well as intense Faraday A-terms observed in MCD spectra of the respective ditopic complexes 1–3.

According to the perimeter model,<sup>28</sup> it is expected that the intensity of the MCD A-term, which corresponds to the low-energy Q-band, should be about an order of magnitude larger compared with the intensities of the MCD A-terms observed in the B-band region. In the case of the completely electronically uncoupled clathrochelate ligand, it is expected that the low-energy band observed in the  $\sim 500$  nm region will have predominantly MLCT character, while more intense bands in the UV regions will correspond to the  $\pi$ – $\pi^*$  transitions. Taking into consideration electronic structure and the extent of the  $\pi$  system of the clathrochelate substituent, it is expected that all MCD A- and B-terms, which correspond to the clathrochelate-

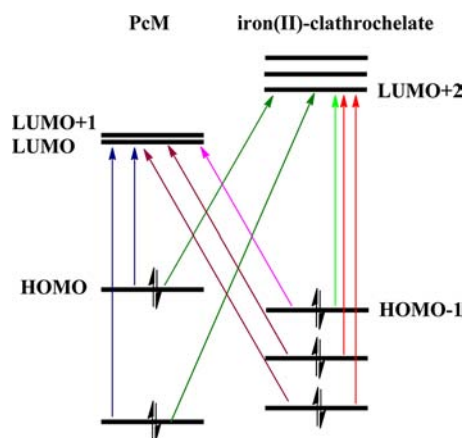


**Figure 6.** Simplified possible types of the transitions in the phthalocyaninoclathrochelates 1–3. Phthalocyanine  $\pi$ – $\pi^*$  transitions are given in blue; phthalocyanine-to-clathrochelate  $\pi$ – $\pi^*$  CT transitions are given in dark green; intra-ligand clathrochelate transitions with significant MLCT are given in light green; clathrochelate  $\pi$ – $\pi^*$  transitions are given in red; clathrochelate-to-phthalocyanine transitions with significant MLCT character are given in magenta; clathrochelate-to-phthalocyanine  $\pi$ – $\pi^*$  transitions are given in brown.

centered MLCT and  $\pi$ – $\pi^*$  transitions will be significantly weaker compared to the MCD signals originating from the electronically allowed transitions of the phthalocyanine core.<sup>30</sup> The tentative analysis of the UV–vis and MCD spectra of phthalocyaninoclathrochelates 1–3 provided above is suggestive of electronically uncoupled phthalocyanine and clathrochelate ligands in these compounds. Further insight into the nature of the experimentally observed transitions was gained using the TDDFT approach. It was found that in general, TDDFT calculations reproduce very well all experimentally observed features in the ditopic phthalocyaninoclathrochelate complexes 1–3 (Figure 7 shows experimental and TDDFT predicted data in  $\text{cm}^{-1}$  scale, while similar data in nm scale are presented in Supporting Information, Figures 3–5). In agreement with the earlier publications,<sup>32,36–39</sup> the absolute TDDFT errors for complexes 1–3 calculated at BP86, B3LYP, and CAM-B3LYP levels are increasing with the increase of the amount of Hartree–Fock exchange but still are in a very reasonable range of  $\sim 0.1$ – $0.3$  eV. Because of the large similarities observed in the experimental UV–vis and MCD as well as TDDFT predicted spectra of the zirconium and hafnium complexes 1 and 2, these will be discussed together. All features in TDDFT calculated spectra of ditopic complexes 1 and 2 could be arranged into five regions as labeled in Figure 7. According to TDDFT calculations, region I, which corresponds to the Q-band region in the experimental spectra of complexes 1 and 2, entirely consists of the phthalocyanine-centered  $\pi$ – $\pi^*$  transitions. These intense transitions originate from the HOMO ( $\pi$ , Pc)  $\rightarrow$  LUMO, LUMO+1 ( $\pi^*$ , Pc) excitations.

In agreement with the TDDFT calculations, the Q-band envelope in UV–vis and MCD spectra of the ditopic complexes 1 and 2 should be dominated by the doubly degenerate (or nearly doubly degenerate)  $\pi$ – $\pi^*$  transitions, which should result in the intense MCD A-terms. It is known that the TDDFT approach tends to underestimate oscillator strengths of the low energy  $\pi$ – $\pi^*$  transitions in phthalocyanines,<sup>32</sup> and thus it is expected that the actual intensities of the predominantly phthalocyanine-centered  $\pi$ – $\pi^*$  transitions in

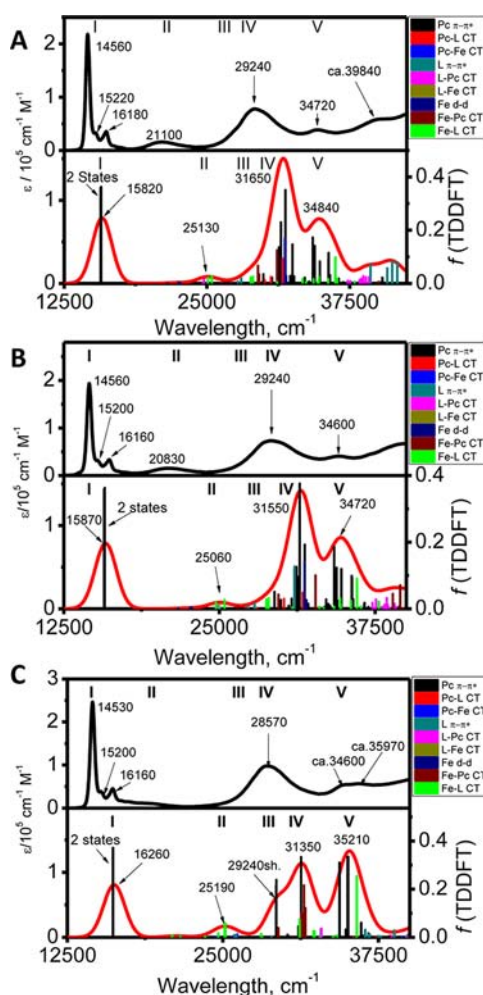


**Figure 7.** Experimental (top) and TDDFT predicted (bottom) UV–vis spectra of hafnium(IV)-capped complex 1 (A), zirconium(IV)-capped complex 2 (B), and lutetium(III)-capped complex 3 (C). Spectral regions are labeled with Roman numbers.

complexes 1 and 2 should be larger than those predicted by the TDDFT.

The region II envelope, which corresponds to the low intensity band centered at  $\sim 480$  nm in the UV–vis spectra of complexes 1 and 2 is dominated by seven excited states. The most intense transitions have charge-transfer character and originate from clathrochelate( $\pi$ ) + iron(d) (HOMO-1 to HOMO-3)  $\rightarrow$  clathrochelate ( $\pi^*$ , LUMO+2 to LUMO+4) transitions. In addition, two lower intensity charge-transfer bands originating from HOMO-1 (clathrochelate( $\pi$ ) + iron-(d)) to LUMO and LUMO+1 (phthalocyanine  $\pi^*$ ) transitions are indicative of the potential weak electronic coupling between phthalocyanine and clathrochelate fragments. This pair of nearly degenerate charge-transfer transitions should result in the weak MCD Faraday A-term, while the other excited states should lead to Faraday B-term in the MCD spectra of 1 and 2.

The TDDFT predicted region III envelope corresponds to the low-energy wing of the B-band region (Figure 7). TDDFT calculations predict eight relatively intense excited states in this region with the most intense excited states being predominantly intra-ligand clathrochelate charge-transfer, intraligand phthalocyanine-centered  $\pi$ – $\pi^*$ , and clathrochelate (L + Fe<sub>d</sub>) to phthalocyanine ( $\pi^*$ ) transitions. Again, the latter transitions are indicative of the potential weak electronic coupling between

phthalocyanine and clathrochelate substituents. The presence of predominantly phthalocyanine-centered  $\pi-\pi^*$  transitions in region III envelope could explain the existence of the weak Faraday A-term experimentally observed in the MCD spectra of complexes **1** and **2** at  $\sim 430$  nm. Following TDDFT calculations, region IV of the UV-vis spectrum consists of  $\sim 40$  excited states with predominantly phthalocyanine-centered  $\pi-\pi^*$  transitions being the most intense. Region V of the TDDFT predicted UV-vis spectra of ditopic complexes **1** and **2** consist of the numerous excited states with clathrochelate- and phthalocyanine-centered intraligand transitions.

The electronic structure of lutetium complex **3** is slightly different from that in complexes **1** and **2**. Specifically, the phthalocyanine-centered HOMO is better separated from the clathrochelate-centered HOMO-1 to HOMO-3 (Figure 4). The phthalocyanine-centered LUMO and LUMO+1 are closer in energy to several clathrochelate centered unoccupied MOs. As a result, TDDFT predicted origins and energies of the excited states in regions I–V (Figure 7) are slightly different compared to those in complexes **1** and **2**. The spectral region I envelope consists of two excited states originating from HOMO ( $\pi$ , Pc)  $\rightarrow$  LUMO, LUMO+1 ( $\pi^*$ , Pc) transitions. These transitions are responsible for the intense Q-band observed in the UV-vis spectrum of complex **3** as well as corresponding very intense Faraday MCD A-term observed in the MCD spectrum of this compound. The spectral region II consists of eight excited states of significant intensity. Five of the most intense transitions predominantly originate from HOMO-1 to HOMO-3 ( $\pi$ , L + d, Fe)  $\rightarrow$  LUMO+2 to LUMO+4 ( $\pi^*$ , L) charge-transfer excitations and (unlike transitions in complexes **1** and **2**) are localized at the clathrochelate ligand. The TDDFT predicted region III spectral envelope is dominated by the two excited states, which have predominant phthalocyanine intraligand  $\pi-\pi^*$  character and are similar to complexes **1** and **2**. These are responsible for the weak Faraday A-term observed in MCD spectrum of complex **3**. Again, similar to ditopic complexes **1** and **2**, region IV of the spectral envelope of lutetium complex **3** is dominated by several phthalocyanine-centered intraligand  $\pi-\pi^*$  transitions.

Overall, experimental UV-vis and MCD spectra as well as TDDFT calculations on the phthalocyaninoclathrochelates **1–3** clearly suggest that their spectra are dominated by the intraligand transitions localized on either the phthalocyanine macrocycle or the clathrochelate fragment. Although TDDFT calculations predict several clathrochelate-to-phthalocyanine and phthalocyanine-to-clathrochelate transitions in UV-vis region, their intensities should be small and thus it is extremely challenging to extract those transitions (if present) from the experimental UV-vis and MCD data. Thus, the questions whether or not clathrochelate ligand is even weakly electronically coupled to the phthalocyanine fragment remains open at this time.

**Oxidation of Phthalocyaninoclathrochelate Complexes at Spectroelectrochemical Conditions.** Redox properties of phthalocyaninoclathrochelates **1–3** have already been investigated by some of us using the cyclic voltammetry (CV) approach in an *o*-DCB/TBAP system (Table 2).<sup>8,9</sup> The redox behavior of the ditopic complexes **1–3** in *o*-DCB/TBAP and DCM/TBAP (system, which was used for spectroelectrochemical experiments described below) is virtually identical, and thus will not be discussed in details.

The first reversible oxidation and reduction processes were attributed to the phthalocyanine core based on the potential

**Table 2. Redox Properties (mV) of the Hybrid Complexes 1–3<sup>a</sup>**

| complex               | Ox3                 | Ox2  | Ox1  | Red1  | Red2  | Red3                 |
|-----------------------|---------------------|------|------|-------|-------|----------------------|
| <b>1</b> <sup>b</sup> | 1700 <sup>irr</sup> | 1260 | 1030 | −650  | −1080 | −1860 <sup>irr</sup> |
| <b>2</b> <sup>b</sup> | 1680 <sup>irr</sup> | 1270 | 1030 | −640  | −1070 | −1870 <sup>irr</sup> |
| <b>3</b> <sup>c</sup> | 1420 <sup>irr</sup> | 990  | 610  | −1090 | −1690 |                      |

<sup>a</sup>*o*-dichlorobenzene; TBAP; Ag/AgCl. <sup>b</sup>Ref 8. <sup>c</sup>Ref 9.

difference and their similarities to the parent hafnium, zirconium, or lutetium phthalocyanine complexes.<sup>12</sup> The second quasi-reversible and the third irreversible oxidation waves at CV conditions were attributed to the oxidation of the clathrochelate substituent based on their similarity to the oxidation processes observed in the parent clathrochelates.<sup>11</sup> In agreement with these tentative assignments, our DFT calculations predict that the HOMO and the LUMO are predominantly phthalocyanine-centered, while HOMO-1 and HOMO-2 have predominantly clathrochelate character. To verify experimental electrochemical assignments and DFT calculation, spectroelectrochemical experiments on all ditopic complexes **1–3** were conducted in the DCM/TBAP system. The spectroelectrochemical transformations of the phthalocyaninoclathrochelate complexes **1–3** are presented in Figure 8 and Supporting Information, Figures 6 and 7. In all cases studied, during oxidation at the first oxidation potential in spectroelectrochemical experiments, initial Q-band intensity at  $\sim 690$  nm and B-band  $\sim 350$  nm decreases, while the three new bands observed at  $\sim 425$ ,  $\sim 530$ , and  $\sim 830$  nm appear in the UV-vis spectra of the ditopic complexes **1–3**. In each case, the first oxidation was accompanied by six isosbestic points and is characteristic of formation of the phthalocyanine-centered cation-radical.<sup>41</sup>

The high intensity of the cation-radical band at  $\sim 830$  nm is characteristic of the monomeric form of the oxidized ditopic complexes **1–3** (i.e.,  $[1-3]^+$ ), while the presence of the weak and broad band at  $\sim 720$  nm is indicative of a small fraction of the  $[1-3]_2^{2+}$  dimers.<sup>41</sup> Such dimers are well-known and originate from the cofacial  $\pi-\pi$  interaction between monomeric  $[1-3]^+$  complexes. It should be noted that in agreement with electrochemical data, the first oxidation process is fully reversible, and the initial neutral phthalocyaninoclathrochelates **1–3** can be regenerated from corresponding cation-radicals upon electrochemical reduction (Supporting Information, Figure 5). During electrolysis at the second oxidation potential, all phthalocyanine-centered cation-radical bands at  $\sim 830$ ,  $\sim 720$ ,  $\sim 530$ ,  $\sim 420$ , and  $\sim 330$  nm lost their intensities (Supporting Information, Figure 6) without formation of the new absorption bands. Since initial neutral complexes **1–3** cannot be regenerated from these doubly oxidized compounds, it easy to conclude that at the relatively slow bulk electrolysis conditions, dications  $[1-3]^{2+}$  are not stable and degrade in solution. This observation is also in agreement with the electrochemical data, which is suggestive of the quasi-reversibility of the second oxidation process only at high scan rates. Overall, spectroelectrochemical data support earlier tentative assignments of the redox properties of phthalocyaninoclathrochelate complexes **1–3** and are in excellent agreement with DFT calculations presented above, which are indicative of a phthalocyanine-centered HOMO.

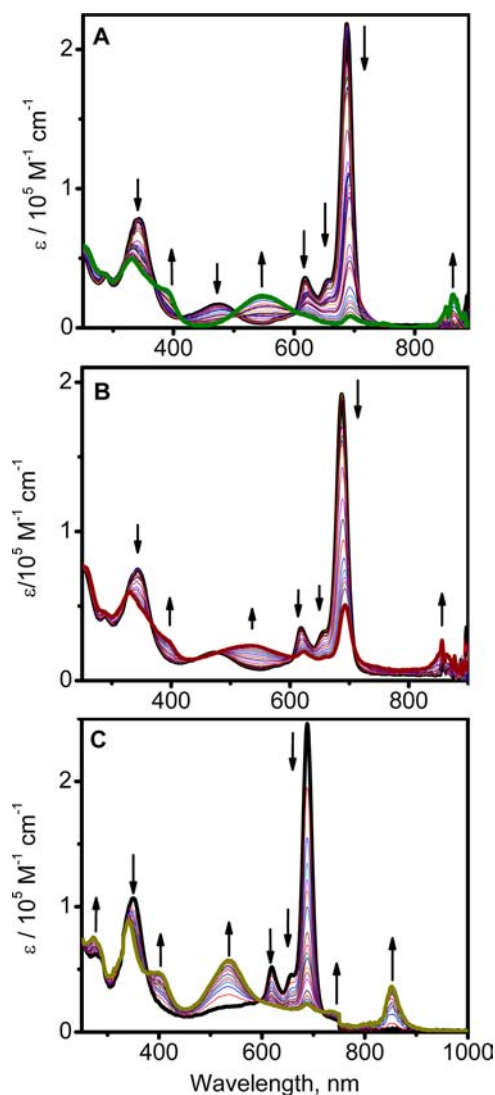


**Figure 8.** Oxidation of the hafnium(IV)-capped complex **1** (A), zirconium(IV)-capped complex **2** (B), and lutetium(III)-capped complex **3** (C) at the first oxidation potential in DCM/TBAP system in spectroelectrochemical experiment.

#### 4. CONCLUSIONS

An insight into the electronic structure of several hafnium(IV), zirconium(IV), and lutetium(III) phthalocyaninoclathrochelates has been discussed on the basis of experimental UV-vis, MCD, electro- and spectroelectrochemical data as well as DFT and TDDFT calculations. Although UV-vis and MCD spectroscopy can be interpreted in the first approximation as a superposition of the phthalocyanine-centered and clathrochelate-centered transitions, theoretical TDDFT predictions revealed a more complex picture. In particular, multiple phthalocyanine-to-clathrochelate and clathrochelate-to-phthalocyanine charge-transfer transitions were predicted in all experimentally observed spectral envelopes, and thus it was concluded that the electronic structure and spectroscopy of the phthalocyaninoclathrochelates can be described as a superposition of the weakly interacting phthalocyanine and clathrochelate substituents. DFT calculations clearly confirm that the HOMO in all tested complexes is localized on the phthalocyanine ligand. In agreement with this prediction, spectroelectrochemical data clearly is suggestive of the

formation of the phthalocyanine-centered cation-radical during electrolysis of all tested phthalocyaninoclathrochelates at the first oxidation potential. It was found that the monomeric cation-radical species dominate in solution over the dimeric cation-radicals. In agreement with the electrochemical data, monitored by the spectroelectrochemical method, electrolysis of one-electron oxidized complexes at the second oxidation potential results in degradation of the phthalocyaninoclathrochelate assembly.

#### ■ ASSOCIATED CONTENT

##### Supporting Information

UV-vis and MCD spectra of nickel tetra-*tert*-butylphthalocyanine; experimental and TDDFT predicted UV-vis spectra of complexes **1–3** in nm scale; spectroelectrochemical reduction of the singly oxidized complexes **1–3**; spectroelectrochemical oxidation of the singly oxidized complexes **1–3** at the second oxidation potential. This material is available free of charge via the Internet at <http://pubs.acs.org>. CCDC 780361 contains the supplementary crystallographic data for this paper. These data can be obtained free of charge via <http://www.ccdc.cam.ac.uk/conts/retrieving.html>, or from the Cambridge Crystallographic Data Centre, 12 Union Road, Cambridge CB2 1EZ, U.K.; fax: (+44) 1223-336-033; or e-mail: [deposit@ccdc.cam.ac.uk](mailto:deposit@ccdc.cam.ac.uk).

#### ■ AUTHOR INFORMATION

##### Corresponding Author

\*E-mail: [vnemykin@d.umn.edu](mailto:vnemykin@d.umn.edu) (V.N.N.), [voloshin@ineos.ac.ru](mailto:voloshin@ineos.ac.ru) (Y.Z.V.).

##### Notes

The authors declare no competing financial interest.

#### ■ ACKNOWLEDGMENTS

Generous support from the NSF CHE-1110455 and NSF MRI CHE-0922366, Minnesota Supercomputing Institute to V.N., and U of M UROP Grant to J.R.S. is greatly appreciated. This research was also supported by the RFBR (Grants 10-03-00837 and 12-03-00961) and RAS (programs 6 and 7).

#### ■ REFERENCES

- (1) (a) Heath, J. R.; Ratner, M. A. *Phys. Today* **2003**, *56*, 43. (b) Chen, J.; Lee, T.; Su, J.; Wang, W.; Reed, M. A. *Encyclopedia of Nanoscience and Nanotechnology* **2004**, *5*, 633. (c) Weiss, J. *Coord. Chem. Rev.* **2010**, *254*, 2247. (d) *Nano and Molecular Electronics Handbook*; Lyshevski, S. E., Ed.; CRC Press: New York, 2007; p 912. (e) Bayley, H. *Nature (London, U. K.)* **2010**, *467*, 164. (f) Giacalone, F.; Martin, N. *Adv. Mater. (Weinheim, Ger.)* **2010**, *22*, 4220. (g) Jurow, M.; Schuckman, A. E.; Batteas, J. D.; Drain, C. M. *Coord. Chem. Rev.* **2010**, *254*, 2297. (h) Chung, A.; Deen, J.; Lee, J.-S.; Meyyappan, M. *Nanotechnology* **2010**, *21*, 412001/1. (i) Belosludov, R. V.; Farajian, A. A.; Baba, H.; Mizuseki, H.; Kawazoe, Y. *Jpn. J. Appl. Phys., Part 1* **2005**, *44*, 2823. (j) Belosludov, R. V.; Farajian, A. A.; Kikuchi, Y.; Mizuseki, H.; Kawazoe, Y. *Comput. Mater. Sci.* **2006**, *36*, 130. (k) Lee, S. U.; Belosludov, R. V.; Mizuseki, H.; Kawazoe, Y. *J. Phys. Chem. C* **2007**, *111*, 15397. (l) Lee, S. U.; Belosludov, R. V.; Mizuseki, H.; Kawazoe, Y. *Small* **2008**, *4*, 962. (m) Lehn, J.-M. *Supramolecular Chemistry*; VCH: Weinheim, Germany, 1995. (n) Balzani, V.; Juris, A.; Venturi, M.; Campagna, S.; Serroni, S. *Chem. Rev.* **1996**, *96*, 759.
- (2) (a) Miller, J. S.; Epstein, A. J. *Angew. Chem., Int. Ed. Engl.* **1994**, *33*, 385. (b) Epstein, A. J.; Miller, J. S. *Synth. Met.* **1996**, *80*, 231. (c) Barlow, S. *Inorg. Chem.* **2001**, *40*, 7047. (d) Barlow, S.; O'Hare, D. *Chem. Rev.* **1997**, *97*, 637. (e) Kaim, W.; Lahiri, G. K. *Angew. Chem., Int. Ed.* **2007**, *46*, 1778. (f) Kaim, W.; Sarkar, B. *Coord. Chem. Rev.* **2007**, *251*, 584. (g) Chisholm, M. H.; Patmore, N. J. *Acc. Chem. Res.*

- 2007, 40, 19. (h) Cowan, D. O.; Kaufman, F. J. *Am. Chem. Soc.* **1970**, 92, 6198. (i) Morrison, W. H., Jr.; Krogsrud, S.; Hendrickson, D. N. *Inorg. Chem.* **1973**, 12, 1998. (j) Venkatasubbaiah, K.; Doshi, A.; Nowik, I.; Herber, R. H.; Rheingold, A. L.; Jakle, F. *Chem.—Eur. J.* **2008**, 14, 444. (k) Venkatasubbaiah, K.; Nowik, I.; Herber, R. H.; Jaekle, F. *Chem. Commun.* **2007**, 2154. (l) Morrison, W. H., Jr.; Hendrickson, D. N. *Inorg. Chem.* **1975**, 14, 2331. (m) Ribou, A.-C.; Launay, J.-P.; Sachtleben, M. L.; Li, H.; Spangler, C. W. *Inorg. Chem.* **1996**, 35, 3735. (n) Patoux, C.; Coudret, C.; Launay, J.-P.; Joachim, C.; Gourdon, A. *Inorg. Chem.* **1997**, 36, 5037. (o) Hadt, R. G.; Nemykin, V. N. *Inorg. Chem.* **2009**, 48, 3982.
- (3) (a) Bucher, C.; Devillers, C. H.; Moutet, J.-C.; Royal, G.; Saint-Aman, E. *Coord. Chem. Rev.* **2009**, 253, 21. (b) Loim, N. M.; Abramova, N. V.; Sokolov, V. I. *Mendeleev Commun.* **1996**, 46. (c) Burrell, A. K.; Campbell, W. M.; Jameson, G. B.; Officer, D. L.; Boyd, P. D. W.; Zhao, Z.; Cocks, P. A.; Gordon, K. C. *Chem. Commun.* **1999**, 637. (d) Rhee, S. W.; Na, Y. H.; Do, Y.; Kim, J. *Inorg. Chim. Acta* **2000**, 309, 49. (e) Kim, J.; Rhee, S. W.; Na, Y. H.; Lee, K. P.; Do, Y.; Jeoung, S. C. *Bull. Korean Chem. Soc.* **2001**, 22, 1316. (f) Shoji, O.; Okada, S.; Satake, A.; Kobuke, Y. *J. Am. Chem. Soc.* **2005**, 127, 2201. (g) Auger, A.; Swarts, J. C. *Organometallics* **2007**, 26, 102. (h) Morisue, M.; Kalita, D.; Haruta, N.; Kobuke, Y. *Chem. Commun.* **2007**, 2348. (i) Nemykin, V. N.; Barrett, C. D.; Hadt, R. G.; Subbotin, R. I.; Maximov, A. Y.; Polshin, E. V.; Kuposov, A. Y. *Dalton Trans.* **2007**, 3378. (j) Nemykin, V. N.; Galloni, P.; Floris, B.; Barrett, C. D.; Hadt, R. G.; Subbotin, R. I.; Marrani, A. G.; Zaroni, R.; Loim, N. M. *Dalton Trans.* **2008**, 4233. (k) Nemykin, V. N.; Rohde, G. T.; Barrett, C. D.; Hadt, R. G.; Bizzarri, C.; Galloni, P.; Floris, B.; Nowik, I.; Herber, R. H.; Marrani, A. G.; Zaroni, R.; Loim, N. M. *J. Am. Chem. Soc.* **2009**, 131, 14969. (l) Galloni, P.; Floris, B.; de Cola, L.; Cecchetto, E.; Williams, R. M. *J. Phys. Chem. C* **2007**, 111, 1517. (m) Nemykin, V. N.; Kobayashi, N. *Chem. Commun.* **2001**, 165. (n) Lukyanets, E. A.; Nemykin, V. N. *J. Porphyrins Phthalocyanines* **2010**, 14, 1. (o) Nemykin, V. N.; Rohde, G. T.; Barrett, C. D.; Hadt, R. G.; Sabin, J. R.; Reina, G.; Galloni, P.; Floris, B. *Inorg. Chem.* **2010**, 49, 7497. (p) Rohde, G. T.; Sabin, J. R.; Barrett, C. D.; Nemykin, V. N. *New J. Chem.* **2011**, 35, 1440. (q) Kadish, K. M.; Xu, Q. Y.; Barbe, J. M. *Inorg. Chem.* **1987**, 26, 2565. (r) Xu, Q. Y.; Barbe, J. M.; Kadish, K. M. *Inorg. Chem.* **1988**, 27, 2373. (s) Maiya, G. B.; Barbe, J. M.; Kadish, K. M. *Inorg. Chem.* **1989**, 28, 2524. (t) Solntsev, P. V.; Sabin, J. R.; Dammer, S. J.; Gerasimchuk, N. N.; Nemykin, V. N. *Chem. Commun.* **2010**, 6581.
- (4) (a) Solomon, E. I.; Sarangi, R.; Woertink, J. S.; Augustine, A. J.; Yoon, J.; Ghosh, S. *Acc. Chem. Res.* **2007**, 40, 581. (b) Xi, B.; Liu, I. P.-C.; Xu, G.-L.; Choudhuri, M. M. R.; DeRosa, M. C.; Crutchley, R. J.; Ren, T. *J. Am. Chem. Soc.* **2011**, 133, 15094. (c) Boyd, D. A.; Cao, Z.; Song, Y.; Wang, T.-W.; Fanwick, P. E.; Crutchley, R. J.; Ren, T. *Inorg. Chem.* **2010**, 49, 11525. (d) Muecke, P.; Linseis, M.; Zalis, S.; Winter, R. F. *Inorg. Chim. Acta* **2011**, 374, 36. (e) Kaim, W.; Lahiri, G. K. *Angew. Chem., Int. Ed.* **2007**, 46, 1778. (f) Kaim, W.; Sarkar, B. *Coord. Chem. Rev.* **2007**, 251, 584. (g) Browne, W. R.; Hage, R.; Vos, J. G. *Coord. Chem. Rev.* **2006**, 250, 1653. (h) D'Alessandro, D. M.; Keene, F. R. *Chem. Rev.* **2006**, 106, 2270. (i) D'Alessandro, D. M.; Keene, F. R. *Chem. Soc. Rev.* **2006**, 35, 424. (j) Crutchley, R. J. *Angew. Chem., Int. Ed.* **2005**, 44, 6452. (k) Distefano, A. J.; Wishart, J. F.; Isied, S. S. *Coord. Chem. Rev.* **2005**, 249, 507. (l) Vlcek, A., Jr. *Chemtracts* **1998**, 11, 104. (m) Vlcek, A., Jr. *Chemtracts* **1995**, 7, 149.
- (5) (a) Zhang, Y.; Cai, X.; Bian, Y.; Jiang, J. *Struct. Bonding (Berlin)* **2010**, 135, 275. (b) Pushkarev, V. E.; Tomilova, L. G.; Tomilov, Yu V. *Russ. Chem. Rev.* **2008**, 77, 875. (c) Ishikawa, N. *Polyhedron* **2007**, 26, 2147. (d) Zhu, P.; Pan, N.; Ma, C.; Sun, X.; Arnold, D. P.; Jiang, J. *Eur. J. Inorg. Chem.* **2004**, 518. (e) Buchler, J. W.; Ng, D. K. P. In *Porphyrin Handbook*; Kadish, K. M., Smith, K. M., Guillard, R., Eds.; Academic Press: New York, 2000; Vol. 3, p 245. (f) Ishikawa, N.; Kaizu, Y. *Coord. Chem. Rev.* **2002**, 226, 93. (g) Ishikawa, N. *J. Porphyrins Phthalocyanines* **2001**, 5, 87.
- (6) (a) Low, P. J. *Dalton Trans.* **2005**, 2821. (b) Lent, C. S.; Isaksen, B.; Lieberman, M. J. *Am. Chem. Soc.* **2003**, 125, 1056. (c) Koepf, M.; Trabolsi, A.; Elhabiri, M.; Wytko, J. A.; Paul, D.; Albrecht-Gary, A. M.; Weiss, J. *Org. Lett.* **2005**, 7, 1279. (d) Cheng, P.-N.; Chiang, P.-T.; Chiu, S.-H. *Chem. Commun.* **2005**, 1285. (e) Steurman, D. W.; Tseng, H.-R.; Peters, A. J.; Flood, A. H.; Jeppesen, J. O.; Nielsen, K. A.; Stoddart, J. F.; Heath, J. R. *Angew. Chem., Int. Ed.* **2004**, 43, 6486. (f) Leigh, D. A.; Morales, M. A. F.; Perez, E. M.; Wong, J. K. Y.; Saiz, C. G.; Slawin, A. M. Z.; Carmichael, A. J.; Haddleton, D. M.; Brouwer, A. M.; Buma, W. J.; Wurpel, G. W. H.; Leon, S.; Zerbetto, F. *Angew. Chem., Int. Ed.* **2005**, 44, 3062.
- (7) (a) Ohkubo, K.; Kotani, H.; Shao, J.; Ou, Z.; Kadish, K. M.; Li, G.; Pandey, R. K.; Fujitsuka, M.; Ito, O.; Imahori, H.; Fukuzumi, S. *Angew. Chem., Int. Ed.* **2004**, 43, 853. (b) D'Souza, F.; Chitta, R.; Gadde, S.; Zandler, M. E.; Sandanayaka, A. S. D.; Araki, Y.; Ito, O. *Chem. Commun.* **2005**, 1279. (c) Sutton, L. R.; Scheloske, M.; Pirner, K. S.; Hirsch, A.; Guldi, D. M.; Gisselbrecht, J.-P. *J. Am. Chem. Soc.* **2004**, 126, 10370. (d) Baran, P. S.; Monaco, R. R.; Khan, A. U.; Schuster, D. I.; Wilson, S. R. *J. Am. Chem. Soc.* **1997**, 119, 8363. (e) Balbinot, D.; Atalick, S.; Guldi, D. M.; Hatzimarinaki, M.; Hirsch, A.; Jux, N. J. *Phys. Chem. B* **2003**, 107, 13273. (f) Zhang, T.-G.; Zhao, Y.; Asselberghs, I.; Persoons, A.; Clays, K.; Therien, M. J. *J. Am. Chem. Soc.* **2005**, 127, 9710. (g) Isosomppi, M.; Tkachenko, N. V.; Efimov, A.; Lemmetyinen, H. *J. Phys. Chem. A* **2005**, 109, 4881.
- (8) Voloshin, Y. Z.; Varzatskii, O. A.; Korobko, S. V.; Chernii, V. Y.; Volkov, S. V.; Tomachynski, L. A.; Pehn'ov, V. I.; Antipin, M. Y.; Starikova, Z. A. *Inorg. Chem.* **2005**, 44, 822.
- (9) Voloshin, Y. Z.; Varzatskii, O. A.; Tomilova, L. G.; Breusova, M. O.; Magdesieva, T. V.; Bubnov, Y. N.; Krämer, R. *Polyhedron* **2007**, 26, 2733.
- (10) (a) McKeown, N. B. *Phthalocyanine Materials: Structure, Synthesis and Function*; Cambridge Univ Press: Cambridge, U.K., 1998; p 200. (b) Moser, F. H.; Thomas, A. L. *The Phthalocyanines*, Vol. 2; CRC Press: Boca Raton, FL, 1983. (c) Erk, P.; Hengelsberg, H. In *The Porphyrin Handbook*; Academic Press: New York, 2003; Vol. 19, pp 105–149. (d) Herbst, W.; Hunter, K. *Industrial Organic Pigments Production, Properties, Applications*, 3rd ed.; Wiley-VCH: Weinheim, Germany, 2004; p 638. (e) Sharman, W. M.; van Lier, J. E. In *The Porphyrin Handbook*; Academic Press: New York, 2003; Vol. 15, pp 1–60. (f) McKeown, N. B. In *The Porphyrin Handbook*; Academic Press: New York, 2003; Vol. 15, pp 61–124. (g) Rodriguez-Morgade, M. S.; de la Torre, G.; Torres, T. In *The Porphyrin Handbook*; Academic Press: New York, 2003; Vol. 15, pp 125–160. (h) Kimura, M.; Shirai, H. In *The Porphyrin Handbook*; Academic Press: New York, 2003; Vol. 19, pp 151–177. (i) Thordarson, P.; Nolte, R. J. M.; Rowan, A. E. In *The Porphyrin Handbook*; Academic Press: New York, 2003; Vol. 18, pp 281–301. (j) *Phthalocyanines: Properties and Applications*; Leznoff, C. C.; Lever, A. B. P., Eds.; VCH Publishers: New York, 1990–1996; Vol. 1–4. (k) Flom, S. R. In *The Porphyrin Handbook*; Academic Press: New York, 2003; Vol. 19, pp 179–190. (l) D'Souza, F.; Ito, O. *Chem. Soc. Rev.* **2012**, 41, 86. (m) Wrobel, D.; Graja, A. *Coord. Chem. Rev.* **2011**, 255, 2555. (n) Zagal, J. H.; Griveau, S.; Silva, J. F.; Nyokong, T.; Bedioui, F. *Coord. Chem. Rev.* **2010**, 254, 2755. (o) Nyokong, T. *J. Porphyrins Phthalocyanines* **2008**, 12, 1005. (p) Nyokong, T.; Bedioui, F. *J. Porphyrins Phthalocyanines* **2006**, 10, 1101.
- (11) (a) Voloshin, Y. Z.; Kostromina, N. A.; Krämer, R. *Clathrochelates: synthesis, structure and properties*; Elsevier: Amsterdam, The Netherlands, 2002; (b) Voloshin, Y. Z.; Dolganov, A. V.; Varzatskii, O. A.; Bubnov, Y. N. *Chem. Commun.* **2011**, 47, 7737.
- (12) (a) Kadish, K. M.; Morrison, M. M. *J. Am. Chem. Soc.* **1976**, 98, 3326. (b) Kadish, K. M.; Caemelbecke, E. V.; Royal, G. In *Porphyrin Handbook*; Kadish, K. M., Smith, K. M., Guillard, R., Eds.; Academic Press: New York, 2000; Vol. 8, pp 1–114.
- (13) (a) Voloshin, Y. Z.; Varzatskii, O. A.; Belov, A. S.; Starikova, Z. A.; Dolganov, A. V.; Magdesieva, T. V. *Polyhedron* **2008**, 27, 325. (b) Voloshin, Y. Z.; Varzatskii, O. A.; Palchik, A. V.; Polshin, E. V.; Maletin, Y. A.; Strizhakova, N. G. *Polyhedron* **1998**, 17, 4315. (c) Voloshin, Y. Z.; Stash, A. I.; Varzatskii, O. A.; Belsky, V. K.; Maletin, Y. A.; Strizhakova, N. G. *Inorg. Chim. Acta* **1999**, 284, 180. (d) Voloshin, Y. Z.; Varzatskii, O. A.; Korobko, S. V.; Antipin, M. Y.; Vorontsov, I. I.; Lyssenko, K. A.; Kochubey, D. I.; Nikitenko, S. G.; Strizhakova, N. G. *Inorg. Chim. Acta* **2004**, 357, 3187.

- (14) Frisch, M. J.; Trucks, G. W.; Schlegel, H. B.; Scuseria, G. E.; Robb, M. A.; Cheeseman, J. R.; Scalmani, G.; Barone, V.; Mennucci, B.; Petersson, G. A.; et al. *Gaussian 09*, Revision A.1; Gaussian, Inc.: Wallingford, CT, 2009.
- (15) Dennington II, R. D.; Keith, T. A.; Milam, J. M. *GaussView 5.0*; SemiChem Inc.: Wallingford, CT, 2008.
- (16) Becke, A. D. *Phys. Rev. A* **1988**, *38*, 3098.
- (17) Perdew, J. P. *Phys. Rev. B* **1986**, *33*, 8822.
- (18) Hay, P. J.; Wadt, W. R. *J. Chem. Phys.* **1985**, *82*, 270.
- (19) (a) Becke, A. D. *J. Chem. Phys.* **1993**, *98*, 5648. (b) Lee, C.; Yang, W.; Parr, R. G. *Phys. Rev. B* **1988**, *37*, 785.
- (20) Yanai, T.; Tew, D.; Handy, N. *Chem. Phys. Lett.* **2004**, *393*, 51–57.
- (21) Nemykin, V. N.; Basu, P. *VMOdes: Virtual Molecular Orbital description program for Gaussian, GAMESS, and HyperChem*, Revision A 7.2; A8.1; University of Minnesota: Duluth, MN, 2003–2010.
- (22) APEX2, Version 1.08; Bruker AXS Inc.: Madison, WI, 2004.
- (23) Sheldrick, G. M. *SADABS v.2.01*, Bruker/Siemens Area Detector Absorption Correction Program; Bruker AXS: Madison, WI.
- (24) Sheldrick, G. M. *SHELXTL v. 5.10*, Structure Determination Software Suite; Bruker AXS: Madison, WI.
- (25) (a) Klotz, M.; Pillai, S.; Kodis, G.; Gust, D.; Moore, T. A.; Moore, A. L.; van Grondelle, R.; Kennis, J. T. M. *J. Am. Chem. Soc.* **2011**, *133*, 7007. (b) Cammidge, A. N.; Nekelson, F.; Hughes, D. L.; Zhao, Z.; Cook, M. J. *J. Porphyrins Phthalocyanines* **2010**, *14*, 1001. (c) Satake, A.; Sugimura, T.; Kobuke, Y. *J. Porphyrins Phthalocyanines* **2009**, *13*, 326. (d) Morisue, M.; Kobuke, Y. *Chem.—Eur. J.* **2008**, *14*, 4993. (e) Bottari, G.; Diaz, D. D.; Torres, T. J. *Porphyrins Phthalocyanines* **2006**, *10*, 1083. (f) Chen, P.; Ma, X.; Liu, M. *Macromolecules* **2007**, *40*, 4780. (g) Martynov, A. G.; Gorbunova, Y. G. *Inorg. Chim. Acta* **2007**, *360*, 122. (h) Tome, J. P. C.; Pereira, A. M. V. M.; Alonso, C. M. A.; Neves, M. G. P. M. S.; Tome, A. C.; Silva, A. M. S.; Cavaleiro, J. A. S.; Martinez-Diaz, M. V.; Torres, T.; Rahman, G. M. A. *Eur. J. Org. Chem.* **2006**, 257. (i) Prall, B. S.; Parkinson, D. Y.; Ishikawa, N.; Fleming, G. R. *J. Phys. Chem. A* **2005**, *109*, 10870. (j) Chen, L. X.; Shaw, G. B.; Tiede, D. M.; Zuo, X.; Zapol, P.; Redfern, P. C.; Curtiss, L. A.; Sooksimuang, T.; Mandal, B. K. *J. Phys. Chem. B* **2005**, *109*, 16598. (k) Dunford, C. L.; Williamson, B. E.; Krausz, E. *J. Phys. Chem. A* **2000**, *104*, 3537.
- (26) (a) Mack, J.; Stillman, M. J. In *Porphyrin Handbook*; Kadish, K. M., Smith, K. M., Guillard, R., Eds.; Academic Press: New York, 2000; Vol. 16, pp 43–116. (b) Nemykin, V. N.; Lukanets, E. A. In *Handbook of Porphyrin Science*, Vol. 3, Kadish, K. M., Smith, K. M., Guillard, R., Eds.; World Scientific: Singapore, 2010; pp 1–323. (c) Fukuda, T.; Kobayashi, N. In *Handbook of Porphyrin Science*, Vol. 9; Kadish, K. M., Smith, K. M., Guillard, R., Eds.; World Scientific: Singapore, 2010; pp 1–644. (d) Mack, J.; Stillman, M. J.; Kobayashi, N. *Coord. Chem. Rev.* **2007**, *251*, 429. (e) Stillman, M.; Mack, J.; Kobayashi, N. *J. Porphyrins Phthalocyanines* **2002**, *6*, 296. (f) Nemykin, V. N.; Volkov, S. V. *Russ. J. Coord. Chem.* **2000**, *26*, 436. (g) Nemykin, V. N.; Tsvadze, A. Yu.; Subbotin, N. B.; Kostromina, N. A.; Volkov, S. V. *Russ. J. Coord. Chem.* **1996**, *22*, 297. (h) Komarov, I. V.; Nemykin, V. N.; Subbotin, N. B. *Appl. Magn. Reson.* **1993**, *4*, 377.
- (27) (a) Voloshin, Y. Z.; Varzatskii, O. A.; Palchik, A. V.; Polshin, E. V.; Maletin, Y. A.; Strizhakova, N. G. *Polyhedron* **1998**, *17*, 4315. (b) Voloshin, Y. Z.; Varzatskii, O. A.; Korobko, S. V.; Maletin, Y. A. *Inorg. Chem. Commun.* **1998**, *1*, 328. (c) Voloshin, Y. Z.; Varzatskii, O. A.; Korobko, S. V.; Antipin, M. Yu.; Vorontsov, I. I.; Lyssenko, K. A.; Kochubey, D. I.; Nikitenko, S. G.; Strizhakova, N. G. *Inorg. Chim. Acta* **2004**, *357*, 3187.
- (28) (a) Waluk, J.; Michl, J. *J. Org. Chem.* **1991**, *56*, 2729. (b) Michl, J. *J. Am. Chem. Soc.* **1978**, *100*, 6801. (c) Michl, J. *J. Am. Chem. Soc.* **1978**, *100*, 6812. (d) Michl, J. *J. Am. Chem. Soc.* **1978**, *100*, 6819.
- (29) (a) Mack, J.; Stillman, M. J. *Coord. Chem. Rev.* **2001**, *219–221*, 993. (b) Mack, J.; Stillman, M. J. In *Porphyrin Handbook*; Kadish, K. M., Smith, K. M., Guillard, R., Eds.; Academic Press: New York, 2003; Vol. 16, pp 43–116. (c) Sripathongnag, S.; Ziegler, C. J.; Dahlby, M. R.; Nemykin, V. N. *Inorg. Chem.* **2011**, *50*, 6902.
- (30) (a) Mason, W. R. *A Practical Guide to Magnetic Circular Dichroism Spectroscopy*; John Wiley & Sons Inc.: New York, 2007. (b) Piepho, S. B.; Schatz, P. N. *Group Theory in Spectroscopy with Applications to Magnetic Circular Dichroism*; John Wiley & Sons Inc.: Toronto, Canada, 1983.
- (31) (a) Stuzhin, P. A.; Pimkov, I. V.; Ul'-Khak, A.; Ivanova, S. S.; Popkova, I. A.; Volkovich, D. I.; Kuz'mitskii, V. A.; Donzello, M.-P. *Russ. J. Org. Chem.* **2007**, *43*, 1854. (b) Dunder, D.; Can, H.; Atilla, D.; Gurek, A. G.; Ozturk, Z. Z.; Ahsen, V. *Polyhedron* **2008**, *27*, 3383. (c) Matsushita, O.; Muranaka, A.; Kobayashi, Y.; Kobayashi, N. *Heterocycles* **2007**, *74*, 321. (d) Kobayashi, N.; Nakajima, S.-I.; Ogata, H.; Fukuda, T. *Chem.—Eur. J.* **2004**, *10*, 6294. (e) Kobayashi, N.; Ogata, H. *Eur. J. Inorg. Chem.* **2004**, 906. (f) Fukuda, T.; Makarova, E. A.; Luk'yanets, E. A.; Kobayashi, N. *Chem.—Eur. J.* **2004**, *10*, 117. (g) Maya, E. M.; Garcia-Frutos, E. M.; Vazquez, J.; Torres, T.; Martin, G.; Rojo, G.; Agullo-Lopez, F.; Gonzalez-Jonte, R. H.; Ferro, V. R.; Garcia de la Vega, J. M. *J. Phys. Chem. A* **2003**, *107*, 2110.
- (32) (a) Nemykin, V. N.; Hadt, R. G.; Belosludov, R. V.; Mizuseki, H.; Kawazoe, Y. *J. Phys. Chem. A* **2007**, *111*, 12901–12913. (b) Peralta, G. A.; Seth, M.; Ziegler, T. *Inorg. Chem.* **2007**, *46*, 9111–9125. (c) De Luca, G.; Romeo, A.; Scolaro, L. M.; Ricciardi, G.; Rosa, A. *Inorg. Chem.* **2009**, *48*, 8493–8507.
- (33) (a) Mack, J.; Kobayashi, N.; Stillman, M. J. *J. Inorg. Biochem.* **2010**, *104*, 310. (b) Kobayashi, N.; Mack, J.; Ishii, K.; Stillman, M. J. *Inorg. Chem.* **2002**, *41*, 5350. (c) Mack, J.; Stillman, M. J. *Inorg. Chem.* **2001**, *40*, 812. (d) Mack, J.; Stillman, M. J. *J. Phys. Chem.* **1995**, *99*, 7935.
- (34) (a) Voloshin, Y. Z.; Varzatskii, O. A.; Palchik, A. V.; Stash, A. I.; Belsky, V. K. *New J. Chem.* **1999**, *23*, 355. (b) Voloshin, Y. Z.; Varzatskii, O. A.; Kron, T. E.; Belsky, V. K.; Zavodnik, V. E.; Palchik, A. V. *Inorg. Chem.* **2000**, *39*, 1907. (c) Voloshin, Y. Z.; Zavodnik, V. E.; Varzatskii, O. A.; Belsky, V. K.; Palchik, A. V.; Strizhakova, N. G.; Vorontsov, I. I.; Antipin, M. Y. *J. Chem. Soc., Dalton Trans.* **2002**, 1193. (d) Voloshin, Y. Z.; Varzatskii, O. A.; Palchik, A. V.; Strizhakova, N. G.; Vorontsov, I. I.; Antipin, M. Y.; Kochubey, D. I.; Novgorodov, B. N. *New J. Chem.* **2003**, *27*, 1148–1155.
- (35) Shannon, R. D. *Acta Crystallogr., Sect. A* **1976**, *32*, 751–767.
- (36) (a) Hieringer, W.; Goeling, A. *Chem. Phys. Lett.* **2006**, *419*, 557. (b) Irgibaeva, I.; Aldongarov, A.; Barashkov, N.; Schmedake, T. *Int. J. Quantum Chem.* **2008**, *108*, 2641. (c) Gritsenko, O.; Baerends, E. J. *J. Chem. Phys.* **2004**, *121*, 655. (d) Dreuw, A.; Head-Gordon, M. *J. Am. Chem. Soc.* **2004**, *126*, 4007. (e) Ziegler, T.; Krykunov, M. *J. Chem. Phys.* **2010**, *133*, 074104/1. (f) Zhekova, H. R.; Seth, M.; Ziegler, T. *J. Phys. Chem. A* **2010**, *114*, 6308. (g) Fan, J.; Autschbach, J.; Ziegler, T. *Inorg. Chem.* **2010**, *49*, 1355. (h) Ziegler, T.; Seth, M.; Krykunov, M.; Autschbach, J. *J. Chem. Phys.* **2008**, *129*, 184114/1. (i) Ziegler, T.; Seth, M.; Krykunov, M.; Autschbach, J.; Wang, F. *J. Chem. Phys.* **2009**, *130*, 154102/1. (j) Nemykin, V. N.; Olsen, J. G.; Perera, E.; Basu, P. *Inorg. Chem.* **2006**, *45*, 3557. (k) Basu, P.; Nemykin, V. N.; Sengar, R. *Inorg. Chem.* **2003**, *42*, 7489. (l) Nemykin, V. N.; Basu, P. *Inorg. Chem.* **2003**, *42*, 4046.
- (37) (a) Semencic, M. C.; Heinze, K.; Foerster, C.; Rapic, V. *Eur. J. Inorg. Chem.* **2010**, 1089. (b) Roy, L. E.; Jakubikova, E.; Guthrie, M. G.; Batista, E. R. *J. Phys. Chem. A* **2009**, *113*, 6745. (c) Romero, T.; Caballero, A.; Espinosa, A.; Tarraga, A.; Molina, P. *Dalton Trans.* **2009**, 2121. (d) Helten, H.; Fankel, S.; Feier-Iova, O.; Nieger, M.; Espinosa Ferao, A.; Streubel, R. *Eur. J. Inorg. Chem.* **2009**, 3226. (e) Pinjari, R. V.; Gejji, S. P. *J. Phys. Chem. A* **2008**, *112*, 12679. (f) Fuentealba, M.; Garland, M. T.; Carrillo, D.; Manzur, C.; Hamon, J.-R.; Saillard, J.-Y. *Dalton Trans.* **2008**, 77. (g) Nemykin, V. N.; Maximov, A. Y.; Kuposov, A. Y. *Organometallics* **2007**, *26*, 3138. (h) Nemykin, V. N.; Makarova, E. A.; Grosland, J. O.; Hadt, R. G.; Kuposov, A. Y. *Inorg. Chem.* **2007**, *46*, 9591. (i) Herber, R. H.; Nowik, I.; Grossland, J. O.; Hadt, R. G.; Nemykin, V. N. *J. Organomet. Chem.* **2008**, *693*, 1850. (j) Nemykin, V. N.; Hadt, R. G. *Inorg. Chem.* **2006**, *45*, 8297–8307. (k) Solntsev, P. V.; Dudkin, S. V.; Sabin, J. R.; Nemykin, V. N. *Organometallics* **2011**, *30*, 3037.
- (38) (a) Venkataramanan, N. S.; Suvitha, A.; Nejo, H.; Mizuseki, H.; Kawazoe, Y. *Int. J. Quantum Chem.* **2011**, *111*, 2340. (b) Balanay, M.

P.; Lee, S. H.; Yu, S.-C.; Kim, D. H. *Bull. Korean Chem. Soc.* **2011**, *32*, 705. (c) Liu, C.-G.; Guan, W.; Song, P.; Yan, L.-K.; Su, Z.-M. *Inorg. Chem.* **2009**, *48*, 6548. (d) Improta, R.; Ferrante, C.; Bozio, R.; Barone, V. *Phys. Chem. Chem. Phys.* **2009**, *11*, 4664. (e) Govind, N.; Valiev, M.; Jensen, L.; Kowalski, K. *J. Phys. Chem. A* **2009**, *113*, 6041. (f) Perun, S.; Tatchen, J.; Marian, C. M. *ChemPhysChem* **2008**, *9*, 282. (g) Nakai, K.; Kurotobi, K.; Osuka, A.; Uchiyama, M.; Kobayashi, N. *J. Inorg. Biochem.* **2008**, *102*, 466. (h) Liao, M.-S.; Watts, J. D.; Huang, M.-J. *J. Phys. Chem. A* **2006**, *110*, 13089. (i) Petit, L.; Quartarolo, A.; Adamo, C.; Russo, N. *J. Phys. Chem. B* **2006**, *110*, 2398. (j) Rosa, A.; Ricciardi, G.; Baerends, E. J.; Zimin, M.; Rodgers, M. A. J.; Matsumoto, S.; Ono, N. *Inorg. Chem.* **2005**, *44*, 6609. (k) Nemykin, V. N.; Hadt, R. G. *J. Phys. Chem. A* **2010**, *114*, 12062.

(39) Nguyen, M. T. D.; Charlot, M.-F.; Aukauloo, A. *J. Phys. Chem. A* **2011**, *115*, 911–922.

(40) Gouterman, M. *J. Mol. Spectrosc.* **1961**, *6*, 138–163.

(41) (a) Gavrilov, V. I.; Konstantinov, A. P.; Derkacheva, V. M.; Luk'yanets, E. A.; Shelepin, I. V. *Zh. Fiz. Khim.* **1986**, *60*, 1448. (b) Nyokong, T.; Gasyna, Z.; Stillman, M. J. *Inorg. Chem.* **1987**, *26*, 1087. (c) Nyokong, T.; Gasyna, Z.; Stillman, M. J. *Inorg. Chem.* **1987**, *26*, 548. (d) Nemykin, V. N.; Chernii, V. Y.; Volkov, S. V. *J. Chem. Soc., Dalton Trans.* **1998**, 2995. (e) Ou, Z.; Zhan, R.; Tomachynski, L. A.; Chernii, V. Y.; Kadish, K. M. *Makroeterotsikly* **2011**, *5*, 164.